Photoactive centers responsible for visible-light photoactivity of N-doped TiO_2†

Caixia Feng, Yan Wang, Zhensheng Jin,* Jiwei Zhang, Shunli Zhang, Zhishen Wu and Zhijun Zhang*

Received (in Montpellier, France) 19th December 2007, Accepted 5th February 2008
First published as an Advance Article on the web 25th March 2008
DOI: 10.1039/b719498f

N-doped TiO_2 (anatase) with high visible light photoactivity was obtained by the thermal treatment of nanotube titanic acid (denoted as NTA) in an NH_3 flow and investigated by means of X-ray diffraction (XRD), transmission electronic microscopy (TEM), diffuse reflectance spectra (DRS), X-ray photoelectron spectroscopy (XPS), electron spin resonance (ESR), and photoluminescence (PL). With increasing NH_3 treatment temperature at T = 400 to 600 °C, the anatase crystallinity of the N-NTA(400–600) samples was gradually enhanced, while at 700 °C a new phase, TiN, appeared in the N-NTA(700) sample. XPS results show that the doped N atoms incorporated into anatase TiO_2 exist in the form of NO. A revised explanation for the triplet ESR signals obtained from the N-NTA(500–700) samples was put forward, *i.e.* the g = 2.004 main peak is contributed by single-electron-trapped oxygen vacancies (denoted as $V_o^{\bullet}$), while two weak peaks (g = 2.023, 1.987) are contributed by chemisorbed NO in well-crystallized anatase TiO_2. The visible light photoactivity is proportional to the height of the g = 2.004 main peak, which suggests that the photoactive centers are $V_o^{\bullet}$-NO–Ti. The adsorbed NO molecule can effectively suppress the photoluminescence of $V_o^{\bullet}$ defects, which facilitates photogenerated charge transfer to the surface reactive centers to conduct redox reactions. The higher the $V_o^{\bullet}$-NO–Ti concentration, the better the visible light photoactivity. The highest photoactivity was obtained for the catalyst, NH_3-treated at 600 °C. But the formation of TiN at T = 700 °C can readily destruct $V_o^{\bullet}$-NO–Ti photoactive centers, and thus readily decreases photoactivity efficiency.

1. Introduction

Titanium dioxide is the most promising photocatalyst for its low cost, non-toxicity, high stability and high efficiency for degradation of difficult-to-remove pollutants. However, it can be activated only by irradiating with ultraviolet (UV) light due to the wide band gap energies, 3.0 eV for the rutile and 3.2 eV for the anatase forms. Therefore, only a small fraction (~5%) of the available solar energy can be utilized in practical applications. To use solar irradiation, many researchers recently have attempted to extend the absorption range of TiO_2 from the ultraviolet (UV) to the visible light region by doping with metal or non-metal elements. Recently, nitrogen-doped TiO_2 has attracted considerable attention due to its photoactivity in the visible region. In 1986, Sato first reported an N-doped TiO_2 photocatalyst with visible light photoactivity prepared by annealing an admixture of NH_4Cl or NH_4OH with titanium hydroxide.[1] Asahi *et al.* obtained visible light active $TiO_{2-x}N_x$ films by sputtering the TiO_2 target in an N_2 (40%)/Ar gas mixture in 2001, which rekindled great attention in TiO_2 as a visible light photocatalyst.[2] Since then, many preparation methods have been reported to dope nitrogen into TiO_2 using different N-doped precursors. Ihara *et al.* prepared a visible light active photocatalyst using the hydrolysis product of $Ti(SO_4)_2$ with an ammonia solution as the N-doped precursor, and evaluated the photoactivity for the oxidation of acetone to CO_2 in the gas phase.[3] Wang *et al.* used the hydrolysis product of tetra-butyl titanate ($Ti(OBu)_4$) with ammonia solution as an N-doped precursor and found visible light photoactivity for the phenol decomposition system.[4] Kisch *et al.* obtained nitrogen-doped titania by mixing titanium tetraisopropoxide with thiourea in ethanol solution as precursor and evaluated the visible light activity by mineralization of the pollutant 4-chlorophenol.[5] On the other hand, Irie *et al.* reported a $TiO_{2-x}N_x$ powder prepared by annealing anatase TiO_2 under an ammonia flow as its photoactivity was evaluated by decomposition of gaseous isopropyl alcohol.[6] Meanwhile, Gole, Burda and co-workers have developed an alternative nanoscale synthesis route that can lead to nitrogen dopant concentrations in excess of 8% in titania.[7–10] They employed the direct nitridation of TiO_2 nanocolloids using alkyl ammonium salts or triethylamine to produce titania-based oxynitride structures at room temperature. Recently, Schmuki and co-wokers have investigated N-doped TiO_2 nanotubes using N-ion implantation and/or an ammonia thermal treatment of TiO_2 nanotubes produced by self-organized electrochemical oxidation of Ti.[11–13] However, there is a question under debate concerning the chemical nature of the

Key Laboratory for Special Functional Materials, Henan University, Kaifeng 475004, P. R. China. E-mail: zhenshengjin@henu.edu.cn; Fax: +86-378-3881358; Tel: +86-378-3881358
† Electronic supplementary information (ESI) available: ESR, XPS and XRD spectra of N-P25(600) and N-P25(700). See DOI: 10.1039/b719498f

photoactive sites responsible for the photoactivity of N-TiO_2 to visible light. Asahi *et al.* proposed that the N doping of TiO_2 shifts the absorption edge of $TiO_{2-x}N_x$ to lower energies and increases the photoactivity in the visible light region through narrowing of the TiO_2 band gap.[2] Some studies, however, proposed that for N-doped anatase TiO_2, the visible light response arises from electronic transitions from localized states to the conduction band.[5,6,14–16] By contrast, the recent study by Serpone and co-workers has proposed that the commonality in all these doped titanias rests with formation of oxygen vacancies and the advent of color centers that absorb the visible light radiation.[17–19]

In 1998, Kasuga *et al.* obtained a nanotube material by treating anatase TiO_2 powders with a 10 mol L^{-1} NaOH aqueous solution at 110 °C for 20 h.[20] Subsequently, Jin[21] and Tsai *et al.*[22] investigated the composition and structure of this nanotube material and concluded that it is nanotube $Na_2Ti_2O_4(OH)_2$, rather than nanotube TiO_2.[20,23] Nanotube $Na_2Ti_2O_4(OH)_2$ can be converted to nanotube titanic acid ($H_2Ti_2O_5{\cdot}H_2O$, denoted as NTA) in a pH = 1 HCl solution, and its crystalline form belongs to the orthorhombic system.[21,22] In 2006, we prepared N-doped TiO_2 by the thermal treatment of NTA in an NH_3 flow and ascribed the visible light response to the formation of the species with triplet ESR signals.[24] However, the origin of the species responsible for the triplet ESR signal is still under discussion. In the present paper, the N-NTA(400–700) samples were investigated by means of XRD, TEM, BET, DRS, XPS, ESR and PL. Based on the discussion of the results, a new explanation is put forward to clarify the effect of doped nitrogen on the visible light photoactivity of N-doped TiO_2. It is suggested that the species with triplet ESR signals are single-electron-trapped oxygen vacancies ($V_o^{\bullet}$) modified by chemisorbed NO in well-crystallized anatase TiO_2.

2. Experimental section

2.1 Sample preparation

300 ml of 40%(w/w) NaOH aqueous solution was placed in a PTFE (polytetrafluoroethylene) bottle, equipped with a reflux condenser. Then, the bottle was placed in an oil bath where the NaOH solution was heated to 110 °C, 5 g of P25-TiO_2(Degussa) powder was added to this mixture which was stirred magnetically. After 24 h, the reaction stopped. When the dispersion cooled down to room temperature, the precipitate, settled from the dispersion, was first washed with de-ionized water to a pH of *ca.* 7.0, and then immersed in a pH = 1.0 HCl solution for 5 h under magnetic stirring, washed again with de-ionized water to remove Cl^-, and dried under vacuum at room temperature. The product obtained was NTA. The as-prepared NTA was then treated in an NH_3 flow for 4 h at different temperatures, T = 400–700 °C, the products obtained are denoted as N-NTA(400–700). Raw P25-TiO_2 was also treated under the same conditions as that of NTA, and the products obtained were denoted as N-P25(400–700).

2.2 Characterization

Transmission electronic microscopy (TEM) images were taken on a JEM-2010 electron microscope. BET surface areas were determined with an ASAP 2010 apparatus produced by Micromeritics. Diffuse reflectance spectra (DRS) were recorded on a Shimadzu U-3010 spectrometer. X-ray diffraction (XRD) patterns were measured by a Philips X'Pert Pro X-ray diffractometer. Photoluminescence (PL) spectra were determined using a SPEX F 212 spectrometer. Electron spin resonance (ESR) spectra were obtained on a Brüker ESP300E apparatus in ambient air. The g-tensors of the ESR signals were obtained by taking g = 2.0036 for diphenyl picryl hydrazyl (DPPH) as a reference. X-ray photoelectron spectroscopy (XPS) characterizations were performed using a Shimadzu Axis Ultra multifunctional X-ray photoelectron spectrometer (Al Kα X-ray, hv = 1486.6 eV). The energy scale of the spectra was corrected using the binding energy of adventitious carbon as C 1s = 284.8 eV; quantitative analysis of the surface elemental composition was accomplished by a computer program using the XPS sensitivity factors provided by the Shimadzu Co.

2.3 Evaluation of photoactivity

The photoactivity of N-NTA(400–700) and N-P25 (400–700) samples was evaluated by photoassisted oxidation of propylene. A 32 ± 2 mg sample was spread on one side of a roughened glass plate (9 × 0.9 × 0.2 cm), which was located in a flat quartz tube reactor. The visible-light source was a 500 W Xenon lamp, which was kept at a distance of 200 mm from the reactor. Between the Xenon lamp and the reactor, a λ = 420 nm cut-off filter and a water cell were inserted to eliminate UV and infrared light, respectively. The intensity of λ ≥ 420 nm irradiating the sample was 0.4 mW cm^{-2}. The feed gas was made up of pure C_3H_6 and dry air, in which the C_3H_6 concentration was equal to 580 ppm V^{-1}, and was stored in a high-pressure cylinder. The concentration of C_3H_6 and carbon dioxide was determined by a chromatographic method (on a Shimadzu GAS CHROMATOGRAPH GC-9A, which was equipped with a GDX-502 column and a hydrogen flame detector, for in-situ analysis). The sensitivity for C_3H_6 analysis was 1 ppm V^{-1}. The flow rate of feed gas was 100 mL h^{-1} C_3H_6 removal = $(C_0-C)/C_0 \times 100\%$.

3. Results and discussion

The XRD patterns of NTA and N-NTA(400–700) are shown in Fig. 1a. Before NH_3 treatment, the crystalline form of NTA belongs to the orthorhombic system. It can be seen that at $T \leq 300$ °C the orthorhombic crystal form remains unchanged. But at T = 400 °C, a phase transformation from orthorhombic to anatase happens. The peak (101) intensity of anatase increases with NH_3 treatment temperature within T = 400–600 °C (see Fig. 1b), which demonstrates that the formation of the crystalline anatase structure is gradually enhanced. However, at T = 700 °C, accompanied with the appearance of the TiN phase (2θ = 37.29°, 43.27°, Fig. 1a), the peak (101) intensity of anatase decreases (see Fig. 1b). The morphologies of as-prepared NTA and N-NTA(400–700) are shown in Fig. 2. As Fig. 2a inset displays, the four-layered nanotube has a structure with inner diameter 6.4 nm, outer diameter 9.3 nm and distance between adjacent layers *ca.* 0.8 nm, the detailed description of its morphology and structure have been reported elsewhere.[21,22,24,25] After treatment under an NH_3

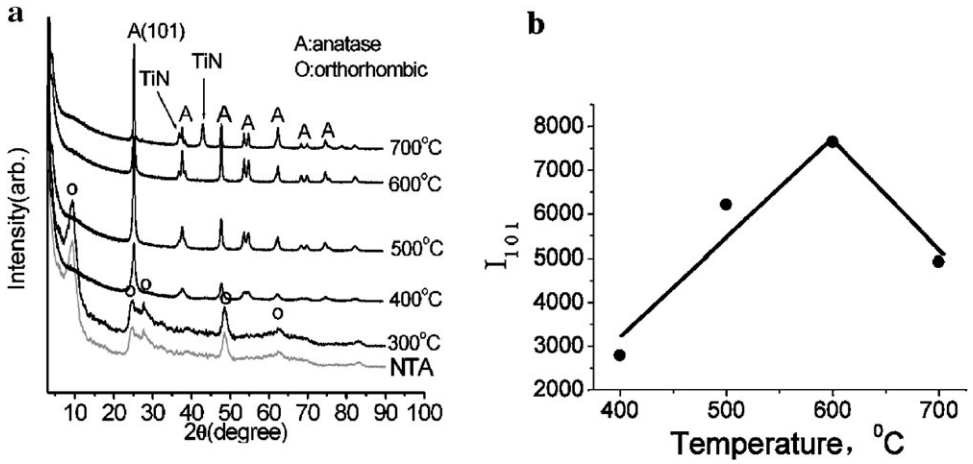

Fig. 1 (a) XRD patterns of NTA and N-NTA(400–700) prepared by treating NTA in an NH_3 flow for 4 h at temperatures of 400–700 °C, respectively. (b) The dependence of peak (101) intensity on NH_3 treating temperature.

flow at T = 400–700 °C, the nanotube morphology breaks and converts into nanobundles (Fig. 2b–e). The BET surface areas change from 379 $m^2\ g^{-1}$ (NTA) to 161, 93, 90, 59 $m^2\ g^{-1}$ for N-NTA(400, 500, 600, 700), respectively, while the nanobundle sizes also become larger from ≈10 nm for N-NTA(400) to ≈30 nm for N-NTA(700) for nanobundles diameters (Fig. 2b–e). The color of the samples changed with NH_3 treating temperature, *i.e.* from white for NTA through gray for N-NTA(400), light yellow for N-NTA(500), yellow for N-NTA(600) to black for N-NTA(700), respectively. These color changes show that the process of dehydration and nitridation reactions during high-temperature NH_3 treatment is very complex.

Table 1 and Fig. 3 demonstrate the changes of visible light photoactivity for N-NTA(400–700) and N-P25(400–700) as a function of NH_3 treating temperature. Both as-prepared NTA and raw P25-TiO_2 are inert. It can be seen from Fig. 3 that the N-NTA(400–700) samples showed higher visible light photoactivity than that of N-P25(400–700). With the increase of NH_3 treating temperature, both series of samples have a maximum propylene removal situated at T = 600 °C, 24.9% for N-NTA(600) and 7.3% for N-P25(600), respectively. The former is 3.4 times that of the latter. The specific surface areas of N-NTA(600) and N-P25(600) equal to 90 and 41 $m^2\ g^{-1}$, respectively, so the ratio of specific activity calculated is 1.5. As T = 700 °C, the activities of both N-NTA(700) and N-P25(700) decrease to close to zero. The inset in Fig. 3 indicates that the dependence of CO_2 production on T. If C_3H_6 was completely oxidized, 1 mole C_3H_6 should produce 3 moles of CO_2. However, the selectivity of CO_2 formation calculated was only *ca.* 80% and 60% for N-NTA(600) and N-P25(600) samples, respectively. This suggests that the visible light photoassisted oxidation of C_3H_6 was incomplete. Comparing to the N-TiO_2 study on the photooxidation of C_2H_4 by Kumar *et al.*,[26] CO_2 produced in incomplete oxidation under visible light illumination was used to evaluate its activity.

The DRS spectra of as-prepared NTA, raw P25-TiO_2 and N-NTA(400–700) are shown in Fig. 4. Compared to NTA and P25-TiO_2, N-NTA(400–700) spectra have a continuous absorption band at $\lambda \geq 400$ nm, but do not possess steep absorption edges in the visible light region. For the DRS spectra of N-NTA(400–700), it can be considered that such visible light absorption might be due to the effect of lattice defects, rather than band to band transitions.[16,27] According to the Kubelka-Munk theory,[28–30]

$$K/S = (1 - R_\infty)^2/2R_\infty \quad (1)$$

where, R_∞ represents reflectance, K and S characterize the losses resulted from absorption and scattering, respectively. If S is independent of wavelength, then the absorptivity (K) is proportional to $(1 - R_\infty)^2/2R_\infty$. Fig. 4 (inset) displays that the absorptivity at 500 nm first decreases and then increases from 400 to 600 °C, as the black-colored N-NTA(700) can absorb nearly all the visible light. If we compare Fig. 4 with Fig. 3, it is obvious that the photoactivity of N-NTA(400–700) has no direct relation with the visible light absorptivity.

Many papers have reported that N-doped TiO_2 prepared by various methods show visible light photoactivity.[1–19] However, the chemical state of the doped nitrogen in the N-TiO_2 lattice is still under discussion. Fig. 5 shows the XPS spectra of N-NTA(400–700) samples for N1s core levels. It can be seen from Fig. 5 that only one kind of N species was detected for the N1s level corresponding to a binding energy of 400.2 eV for the N-NTA(400–600), which Asahi *et al.*[2] and Schmuki *et al.*[13] have assigned to be molecularly chemisorbed γ-N_2. Sato *et al.*, however, believed that this is implausible because molecular N_2 cannot be chemisorbed on metal oxides such as TiO_2 at room temperature.[31] Gole, Burda *et al.*[7–10] studied their N-doped TiO_2 samples prepared by direct nitridation using alkylammonium salts or triethylamine, also pointed out the miss-assignment of the 400 eV XPS peak to molecular N_2 by Asahi,[2] and assigned the peak centered in the range 400.7–401.3 eV obtained by them to N in Ti–O–N bonding.[7–10] Rodriguez *et al.* studied the interaction of NO_2 with Zn by XPS and assigned an N1s peak at 400 eV to be adsorbed NO.[32] Summarizing the references,[7–10,31–33] we can conclude that the preparation methods and conditions used to form N-doped TiO_2 affect the XPS spectral features for nitrogen and that the N1s peak energy value for NO varies within a

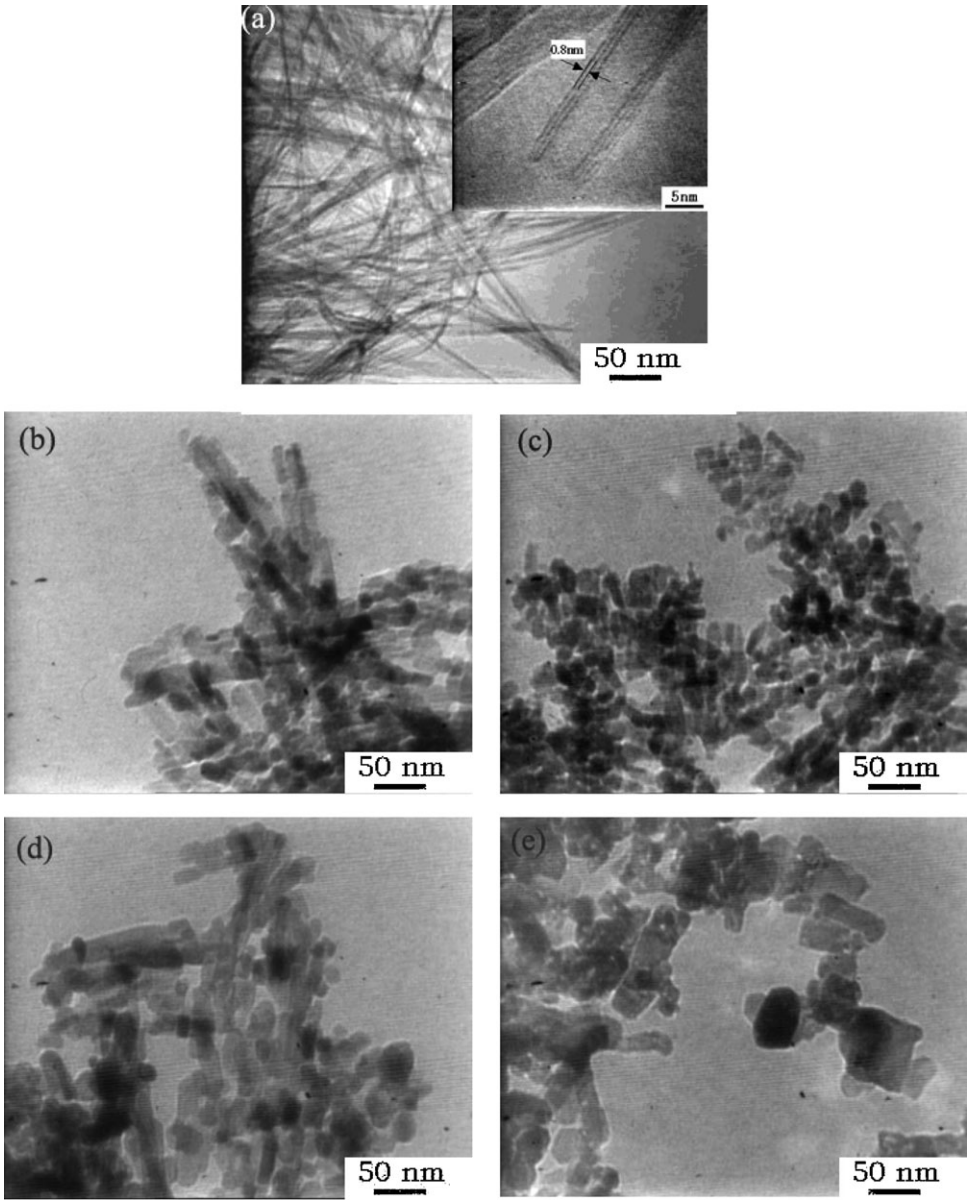

Fig. 2 TEM pictures of NTA and N-NTA(400–700) prepared by treating NTA in an NH_3 flow for 4 h at temperatures of 400–700 °C, respectively: (a) NTA; (b) N-NTA400; (c) N-NTA500; (d) N-NTA600; (e) N-NTA700.

range of 400 to 401.3 eV. E_b(N1s) = 400.2 eV given by us in Fig. 5a–c should be confirmed to be N in NO. When the NH_3 treatment temperature increased to 700 °C, a strong N1s peak at E_b(N1s) = 396.4 eV emerged (Fig. 5d). Many researchers have reported that the N1s peak centered at 396–397 eV should be assigned to an N bound to Ti.[6,34–37] The above results thus imply that, at T = 400–600 °C, NH_3 reacted with the O atom of NTA to form NO, at T = 700 °C, NH_3 mainly reacted with the Ti atom of NTA to produce a new phase TiN (Fig. 1), while the NO formation is dramatically reduced (Fig. 5d).

Table 1 Visible light photoactivity of N-NTA(400–700) and N-P25(400–700)

NH_3 treating temperature °C		400	500	600	700
C_3H_6 removal, %	N-NTA	12.6	21.0	24.9	0
	N-P25	0	3.1	7.3	0.36
CO_2/C_3H_6 mole ratio	N-NTA	1	1.5	2.4	0
	N-P25	0	1.3	1.9	1

Table 2 and Fig. 5e show the change of surface nitrogen concentration with T. Comparing Fig. 3 with Fig. 5e, we can find that there is no direct relationship between the visible light photoactivity and surface nitrogen concentration of N-NTA(400–700). To the contrary, the smaller the surface nitrogen doping, the higher the photoactivity for N-NTA(600). Accompanying the formation of the TiN phase (surface N concentration reaches 11.92%), the photoactivity of N-NTA(700) is lost, which is in agreement with Diwald's results that Ti–N bonding contributes negatively to visible light photoactivity.[37] Since Ti–N bonding is not involved in N-NTA(400–600 °C), the expectation that the valence band

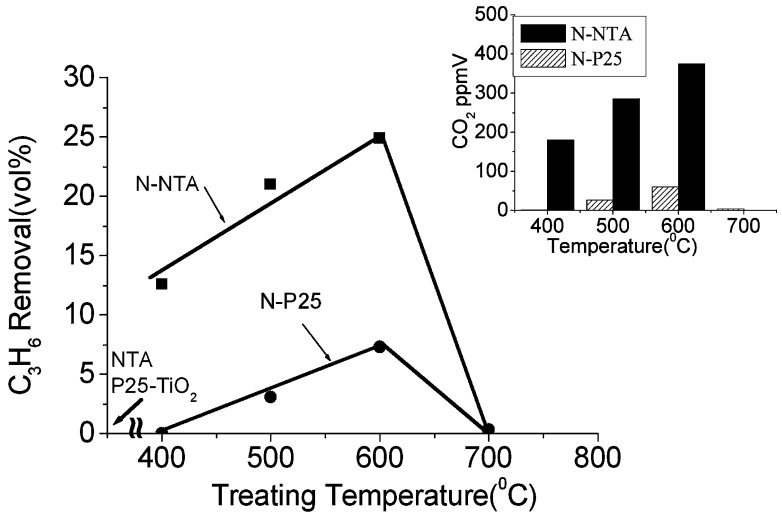

Fig. 3 Visible light photoactivity of N-NTA(400–700) and N-P25(400–700) evaluated by C_3H_6 removal(vol%). Inset: Change of CO_2 production with NH_3 treating temperature.

will be shifted in the negative direction by mixing N2p and O2p states to narrow the band gap is impossible to realize. This point was also proposed by Serpone *et al.*[17] and Majima *et al.*[38] Table 2 shows that the N/O and N/Ti atomic ratios of N-NTA change greatly, while the O/Ti atomic ratios remain within 3.2 ± 0.2. Fig. 6a–c indicate that the oxidation state of Ti in N-NTA(400, 500, 600) samples is identical to Ti^{4+} with $E_b(Ti2p_{3/2})$ = 458.9 eV.[39] But in the deconvolution spectrum of N-NTA(700) (Fig. 6d), a new peak at $E_b(Ti2p_{3/2})$ = 457 eV appears, which represents Ti in Ti–N bond.[34]

It is well known that metal-ion doping can extend the spectral response of TiO_2 into the visible light region from the ultraviolet.[40–44] Sato *et al.* suggested that the role of NO contained in N-doped TiO_2 is similar to that of metal-ion sensitization because the doped N is in an oxidized state in NO.[31] The oxygen vacancies within the TiO_2 lattice can also lead to visible light absorption.[45,46] Using a helium-atom model, Cronemeyer had calculated the ionization energies

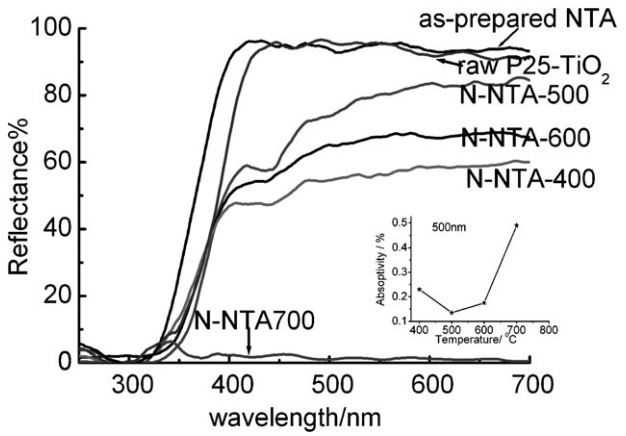

Fig. 4 UV-visible diffuse reflectance spectra of NTA, P25-TiO_2 and N-NTA(400–700) prepared by treating NTA in an NH_3 flow for 4 h at temperatures of 400–700 °C, respectively. Inset: change of visible light absorptivity at 500 nm with NH_3 treating temperature.

for a two-electron-trapped oxygen vacancy (effective charge = 0, denoted as $V_o^{\times}$) in rutile TiO_2.[47] The ionisation energy for the first electron (E_1) equals 0.73 eV (upwards toward the bottom of conduction band, experimental value = 0.75 eV); the ionization energy for the second electron (E_2), *i.e.* at the level of a single-electron-trapped oxygen vacancy (denoted as $V_o^{\bullet}$), is calculated to be 1.64 eV (experimental value = 1.18 eV). E_1 can be moved towards the bottom of conduction band (E_{cb}) with the increase of oxygen-vacancy concentration (N_d):[48]

$$E_{cb} - E_1 = 0.75 - 2.88 \times 10^{-9} N_d^{1/3} \quad (2)$$

In eqn (2), when $N_d = 1.9 \times 10^{25}$ m^{-3}, $E_{cb} - E_1 = 0$. The weight loss of NTA treated at $T \geq 400$ °C to convert to TiO_2 is *ca.* 17%,[49] the oxygen-vacancy concentration (N_d) estimated in the TiO_2 lattice is $>1.9 \times 10^{25}$ m^{-3}, which means: (i) E_1 is immersed in the conduction band; (ii) only the levels of $V_o^{\bullet}$ (E_2) remain in the band gap of TiO_2. TiO_2 has a high dielectric constant.[47] The *g* factor of electrons trapped in the oxygen vacancies of TiO_2 converges to that of free electrons (2.0036), and a number of papers have reported that TiO_2 with $V_o^{\bullet}$ shows a characteristic ESR signal at $g = 2.003 \pm 0.001$.[50–53] The symbol $V_o^{\bullet}$ is also called on F-center.

Oxygen vacancies co-existing with two Ti^{3+} sites in TiO_2 can be obtained by H_2 reduction or by vacuum outgassing at high temperature.[45,46] Such oxygen vacancies are easily re-occupied by the oxygen in the atmosphere. In our previous work, we have found that TiO_2 (anatase) prepared by treating NTA in ambient air contains a large amount of $V_o^{\bullet}$ sites,[26,30,49,54] which were very stable in air atmosphere. By means of a visible-light photoluminescence study on this novel TiO_2, Qian *et al.* found that a sub-band forms within its band gap (sub-band width equals 0.48 eV).[53] Wang *et al.* reported that this novel TiO_2 is responsive to visible light, but it is inactive for the visible-light photocatalytic oxidation of C_3H_6.[55] Here a question is raised: Why is N-NTA(400–600) (*i.e.* N-doped anatase TiO_2) obtained by treating NTA in an

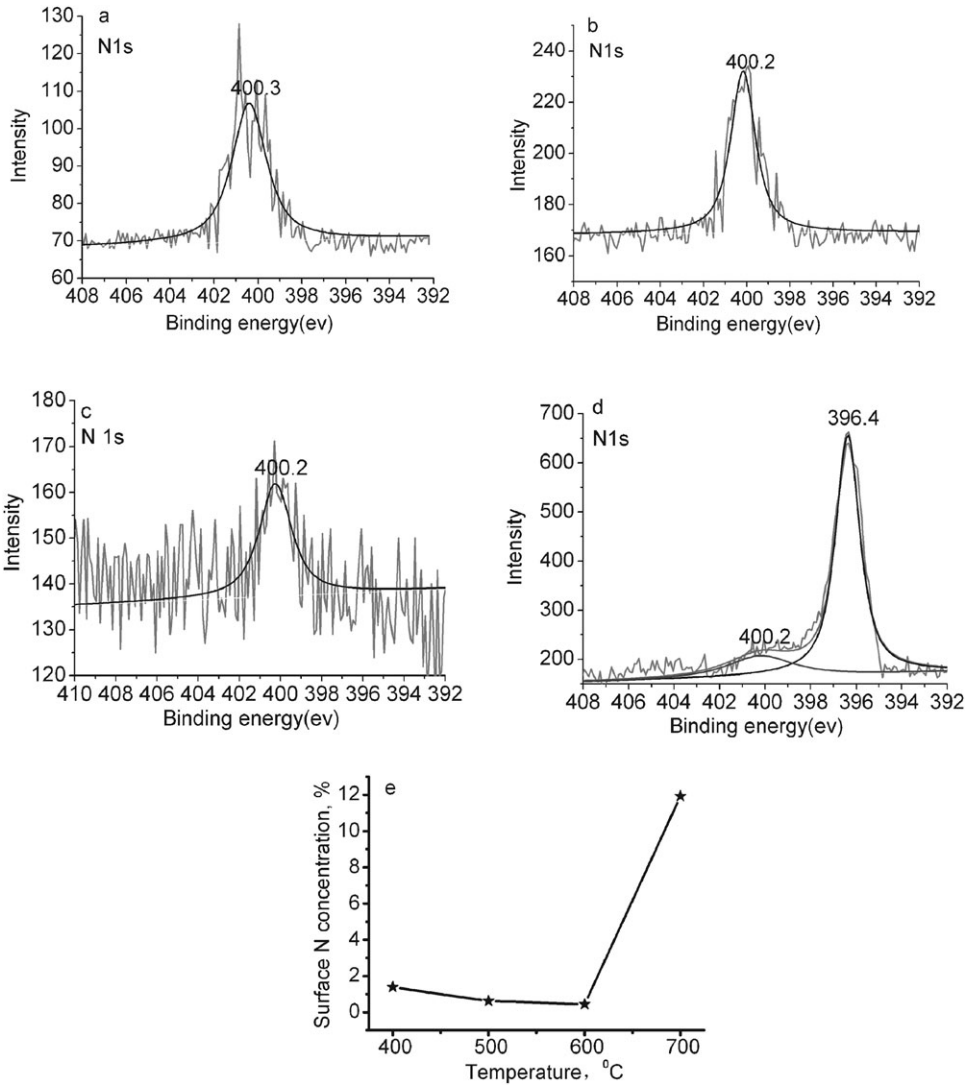

Fig. 5 N1s XPS spectra of N-NTA(400–700) prepared by treating NTA in an NH_3 flow for 4 h at temperatures of 400–700 °C, respectively: (a) N-NTA400 (centered at 400.3 eV); (b) N-NTA500 (centered at 400.2 eV); (c) N-NTA600 (centered at 400.2 eV); (d) N-NTA700 (peaking at 400.2 and 396.4); (e) dependence of surface N concentration on NH_3 treating temperature.

NH_3 flow not only responsive to visible light but also shows a high visible-light photoactivity (Fig. 3)? Shown in Fig. 7 are ESR spectra of N-NTA(400–700) samples. One can see that N-NTA(400) displays a symmetrical ESR peak centered at 3484G, g = 2.004, H (peak width) = 6G (Fig. 7a), which represents the characteristic $V_o^{\bullet}$. This feature suggests that when air atmosphere for the thermal treatment of NTA was replaced by NH_3 at T = 400 °C, $V_o^{\bullet}$ also formed in TiO_2 (anatase). Accompanying this, as the NH_3 treatment temperature increased to 500 °C and 600 °C, the intensity of the g = 2.004 peak (h) is enhanced, and at the same time two weak peaks (3454G, g = 2.023; 3516G, g = 1.987) appear at its both sides of the major peak (Fig. 7b and c). The distance from the weak peaks to the g = 2.004 peak center is 32 ± 1 G. Different assignments for such a triplet displayed by TiO_2, which was prepared by hydrolyzing $TiCl_4$ with aq. NH_3 and then treating under referring conditions, have been reported. In 1966, Iyengar and coworkers assigned the triplet to surface adsorbed O_2^+ species.[56] In 1968, Fukuzawa *et al.* assigned it to a solid-state defect.[57] In 1971, the triplet was re-studied by Iyengar *et al.* and its assignment was modified to be some paramagnetic nitrogen oxides (NO, NO_2, NO_2^-, NO_2^{2-}).[58] In 2005, Prokes *et al.*[10] reported the surface modification of TiO_2 nanostructures to incorporate nitrogen and form visible light absorbing titanium oxynitride centers, ESR performed on these samples identified a resonance at g = 2.0035, which was attributed to an oxygen hole center created near the surface of the nanocolloid. Recently, Giamello *et al.*[59]

Table 2 Surface atomic concentration of N-NTA(400–700)

NH_3 treating temperature °C	400	500	600	700
O, %	75.73	74.93	74.70	68.07
Ti, %	22.87	24.42	24.85	20.01
N, %	1.39	0.66	0.44	11.92
N/Ti	0.061	0.027	0.018	0.60
N/O	0.018	0.009	0.006	0.18
O/Ti	3.3	3.1	3.0	3.4

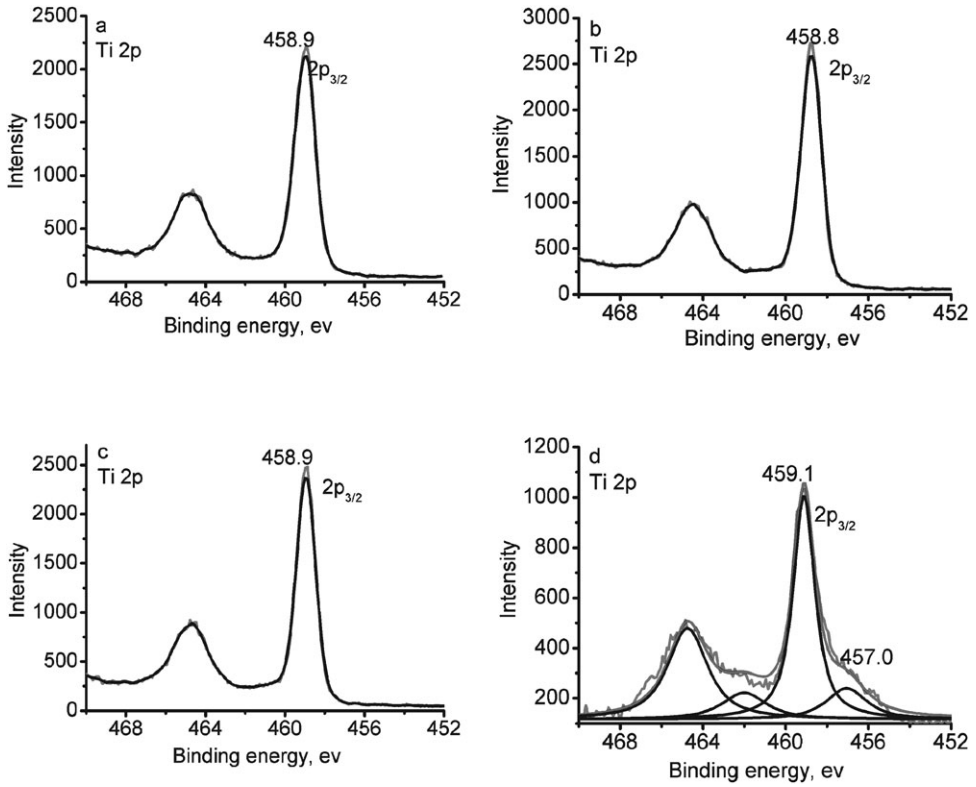

Fig. 6 XPS spectra (Ti 2p) of N-NTA(400–700) prepared by treating NTA in an NH_3 flow for 4 h at temperatures of 400–700 °C, respectively. (a) N-NTA400; (b) N-NTA500; (c) N-NTA600; (d) N-NTA700.

reported the existence of two different triplet ESR signals for N-TiO_2 samples, which were prepared by mixing a solution of titanium(IV) isopropoxide in isopropyl alcohol with a solution of NH_4Cl in water. The sample was then dried and calcinated in air. Giamello *et al.* assigned the first feature as molecular NO permanently trapped in the crystal and the second to a nitrogen based paramagnetic center (NO_2^{2-}). Livraghi *et al.* investigated N-TiO_2 (anatase), prepared by the same method as Giamello *et al.*,[59] with a combined experimental (ESR, DRS) and a theoretical approach.[16] They assigned the triplet signal to be a unique signal of $N^{\bullet}$, that is split into three peaks by the hyperfine interaction of the unpaired electron with the nucleus of one single N atom, and proposed that the origin of photoactivity of N-doped TiO_2 is $N^{\bullet}$ centers. But in this paper, Livraghi *et al.* did not show us XPS results about the chemical state of N with O and Ti in N-TiO_2. And some unpublished results about N-P25(600–700) obtained by us suggest that it is not proper to assign the triplet signal to be a unique signal of $N^{\bullet}$ (see supplementary material†).

Systematically considering the characterization of the results of N-NTA(400–700), here we put forward a new explanation for the triplet ESR signals shown in Fig. 7b–d. The $g = 2.004$ main peak in the triplet is contributed by $V_o^{\bullet}$. The motion of an unpaired electron trapped in an oxygen vacancy will be inevitably modified by the interrelated crystal field and adsorbed polar molecules. The synergistic action of TiO_2 crystallinity and chemisorbed NO on $V_o^{\bullet}$ could be the reason for the formation of two weak peaks ($g = 2.023$, 1.987) superposed on the $V_o^{\bullet}$ signal: (i) although the surface NO concentration of the sample N-NTA(400) is higher (Table 2, N atomic% = 1.39), no weak peaks appear (Fig. 7a). This is likely due to the poor anatase crystallinity (Fig. 1); (ii) for samples N-NTA(500) and N-NTA(600), the anatase crystallinity becomes well defined (Fig. 1), though the surface NO concentrations are less than N-NTA(400) (Table 2), two weak peaks form. Early in 1981, on 500 °C-vacuo-reduced TiO_2, Serwicka *et al.* have found the interaction between $V_o^{\bullet}$ ($g = 2.003$) and adsorbed molecules with high electron affinity at room temperature.[50] After adsorption of O_2, SO_2, $C_6H_5NO_2$ and SF_6, the symmetrical ESR signal at $g = 2.003$ enhanced, while the Ti^{3+} signal ($g = 1.95$) greatly reduced or disappeared. Interestingly, the adsorption of $C_6H_5NO_2$ on 500 °C-vacuo-reduced TiO_2 clearly demonstrated a triplet ESR spectrum at room temperature, and they assigned the triplet as the superposition of $V_o^{\bullet}$ and $C_6H_5NO_2^{-}$ signals.

Comparing Fig. 3 with Fig. 7, it can be seen that the visible light photoactivity of N-NTA(400–700) is obviously correlated with the intensity of the $g = 2.004$ peak (h), which implies that the $V_o^{\bullet}$ defects formed in a well crystallized TiO_2 surface layer and accompanied with chemisorbed NO should be a key structure for the appearance of visible-light photoactivity. Scheme 1 describes the photoactive centre $V_o^{\bullet}$-NO–Ti, where NO is an interstitial molecule between $V_o^{\bullet}$ and Ti in anatase TiO_2, and an O atom in NO links to Ti. Generally speaking, the lattice defects, $V_o^{\bullet}$, of a

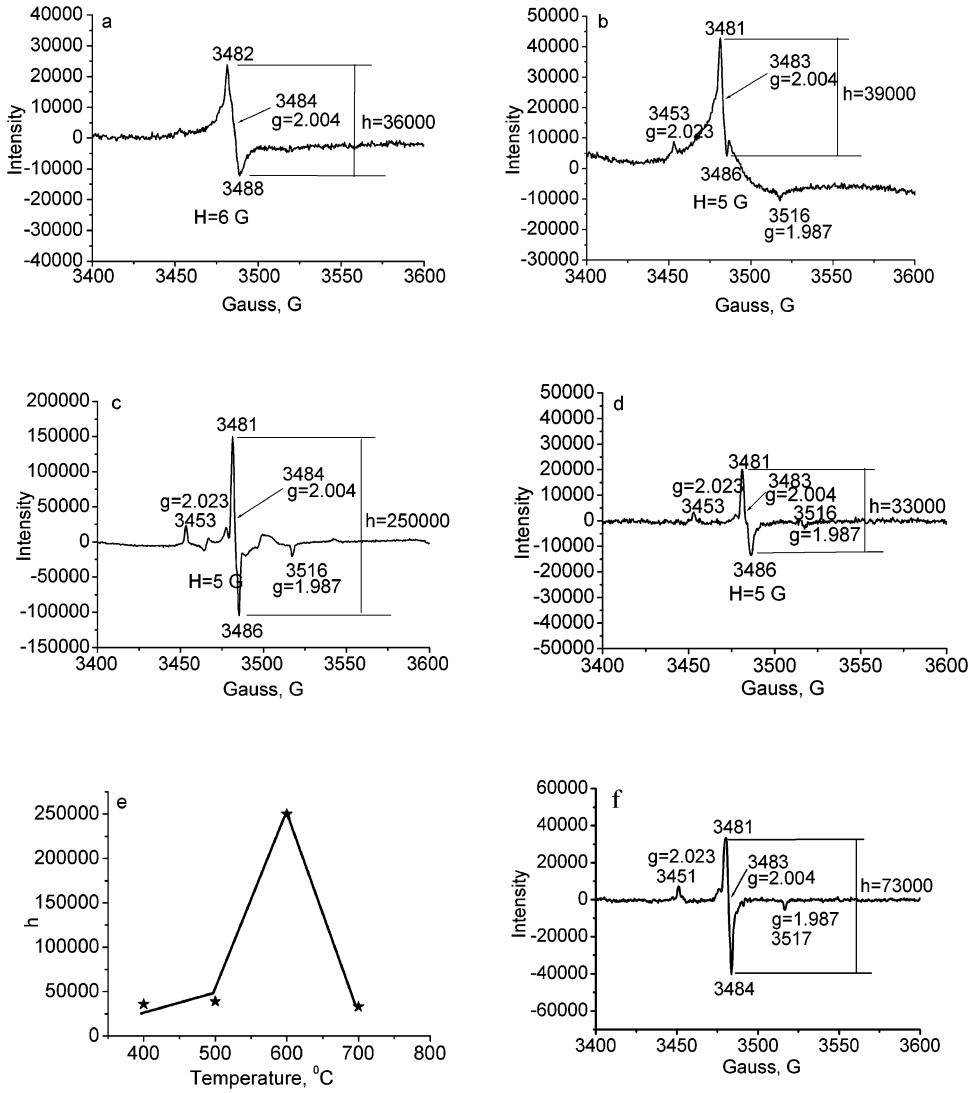

Fig. 7 ESR spectra of N-NTA(400–700) prepared by treating NTA in an NH_3 flow for 4 h at temperatures of 400–700 °C, respectively: (a) N-NTA(400); (b) N-NTA(500); (c) N-NTA(600); (d) N-NTA(700); (e) Dependence of $g = 2.004$ peak height (h) of N-NTA on NH_3 treating temperature; (f) N-P25(600).

semiconductor play the role of recombination centers for photogenerated charges which emit a photon or heat. So, as stated above, TiO_2, with $V_o^{\bullet}$ but without NO, obtained by thermal treatment of NTA in air atmosphere does not exhibit visible light photoactivity. The results shown in Fig. 8 and 3 indicate that the photoluminescence intensities [$I_{PL}(400) > I_{PL}(500) > I_{PL}(600)$, at $\lambda_{ex} = 470$ nm] are in a reverse correlation to the photoactivity. This phenomenon suggests that the interstitial NO between $V_o^{\bullet}$ and Ti can suppress the photoluminescence of $V_o^{\bullet}$ defects. Emeline *et al.* also found that the role of N-doping lies in the stabilization of some defects (color centers) as a result of the defect charge compensation effect.[19] Under these circumstances, the photogenerated charges can transfer to surface reactive sites to conduct redox reactions. The energy relation for the N-doped TiO_2 photocatalytic redox processes is shown in Scheme 2. The lattice defects $V_o^{\bullet}$ generated during NH_3 treatment form a sub-band within the band gap of TiO_2 (anatase), which results in visible light absorption.

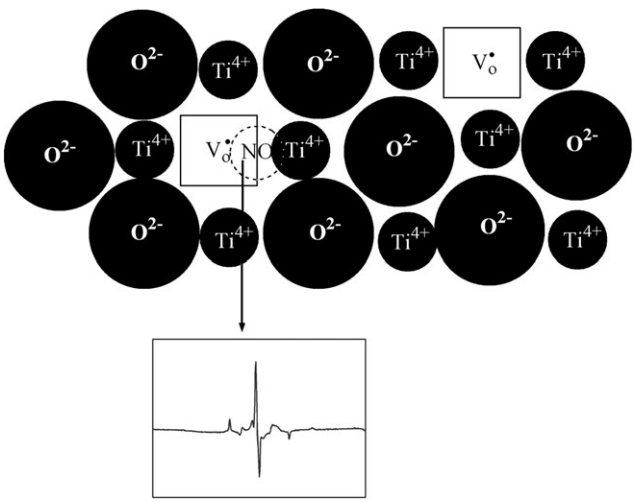

Scheme 1 The model for photoactive center of $V_o^{\bullet}$-NO–Ti: NO is an interstitial molecule between $V_o^{\bullet}$ and Ti in anatase TiO_2, and an O atom in NO links to Ti.

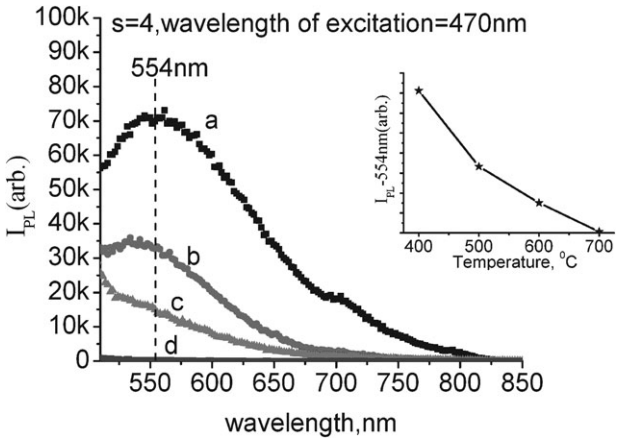

Fig. 8 Photoluminescence spectra of N-NTA(400–700) prepared by treating NTA in an NH_3 flow for 4 h at temperatures of 400–700 °C, respectively: (a) N-NTA400; (b) N-NTA500; (c) N-NTA600; (d) N-NTA700. Inset: dependence of the photoluminescence intensity on temperature (I_{ex} = 470 nm, I_{pl} = 554 nm).

Based on above discussion, the formula for the NH_3 treatment of NTA at T = 400–600 °C may be written as:

$$H_2Ti_2O_5 \cdot H_2O \text{ (orthorhombic)} \xrightarrow{-H_2O} TiO_{2-x}(V_o^{\bullet})_x \text{ (anatase)} \quad (3)$$

$$TiO_{2-x}(V_o^{\bullet})_x \xrightarrow{NH_3} TiO_{2-x-y}(V_o^{\bullet})_x + y(NO)_y \quad (4)$$

The reaction takes two steps: (i) accompanying the dehydration, NTA converts from the orthorhombic form to anatase $TiO_{2-x}(V_o^{\bullet})_x$; (ii) NH_3 reacts with an oxygen atom of $TiO_{2-x}(V_o^{\bullet})_x$ to form NO with an additional $V_o^{\bullet}$, NO will be chemisorbed in the vicinity of $V_o^{\bullet}$.

At T = 700 °C, a transition temperature for the NH_3 treatment of NTA, TiN forms (formula 5). Though TiN can strongly absorb visible light (Fig. 4), it is inert for the photo-assisted oxidation of C_3H_6 (Fig. 3):

$$TiO_{2-x}(V_o^{\bullet})_x \xrightarrow{NH_3} Ti_{1-y}O_{2-x}(V_o^{\bullet})_x(TiN)_y \quad (5)$$

Why is the photoactivity of N-NTA(400–600) higher than that of N-P25(400–600) (see Fig. 3)? It may be that $TiO_{2-x}(V_o^{\bullet})_x$ is chemically more active than P25-TiO_2, and that reaction (4) takes place more easily to form $V_o^{\bullet}$-NO–Ti centers. The intensity of the g = 2.004 peak for N-NTA(600) (Fig. 7c, h = 250 000) is *ca.* 3.4 times of that for N-P25(600) (Fig. 7f, h = 73 000), in accordance with the ratio of their apparent visible light photoactivity.

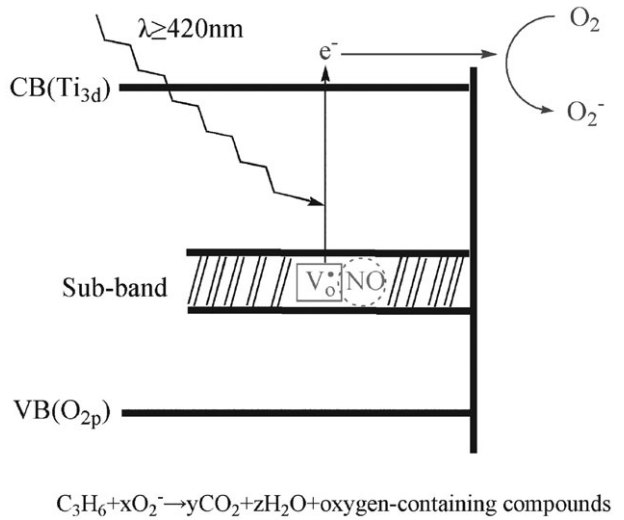

Scheme 2 Schematic illustration of the energy bands for N-TiO_2 together with photocatalytic redox processes. CB, conduction band; VB, valence band. The lattice defects $V_o^{\bullet}$ form a sub-band within the band gap of TiO_2 (anatase), which results in visible light response.

4. Conclusion

N-doped TiO_2 (anatase) with high visible light photoactivity was obtained by treating nanotube titanic acid (NTA) in an NH_3 flow at T = 400–600 °C, as a large amount of $V_o^{\bullet}$ defects form a sub-band within $E_g(TiO_2)$ to extend the optical absorption of N-doped TiO_2 samples into the visible region. The doped nitrogen was in the form of NO and contained in well-crystallized TiO_2. The photoactive centers $V_o^{\bullet}$-NO–Ti can effectively suppress the PL properties of $V_o^{\bullet}$ defects so as to facilitate photogenerated charge transfer to the surface reactive sites to conduct redox reactions, where NO is the interstitial molecule between $V_o^{\bullet}$ and Ti in anatase TiO_2, and the O atom in NO links to Ti. This could suggest that the higher the $V_o^{\bullet}$-NO–Ti concentration, the better the visible light photoactivity.

Acknowledgements

The authors acknowledge the support of the National Natural Science Foundation of China (Grant No. 20071010). Also, the authors are indebted to Prof. Chen Jingrong for the measurement and discussion of ESR data.

References

1 S. Sato, *Chem. Phys. Lett.*, 1986, **123**, 126.
2 R. Asahi, T. Morikawa, T. Ohwaki, K. Aoki and Y. Taga, *Science*, 2001, **293**, 269.
3 T. Ihara, M. Miyoshi, Y. Iriyama, O. Matsumoto and S. Sugihara, *Appl. Catal., B*, 2003, **42**, 403.
4 Z. P. Wang, W. M. Cai, X. T. Hong, X. L. Zhao, F. Xu and C. G. Cai, *Appl. Catal., B*, 2005, **57**, 223.
5 S. Sakthivel, M. Janczarek and H. Kisch, *J. Phys. Chem. B*, 2004, **108**, 19384.
6 H. Irie, Y. Watanabe and K. Hashimoto, *J. Phys. Chem. B*, 2003, **107**, 5483.
7 C. Burda, Y. Lou, X. Chen, A. C. S. Samia, J. Stout and J. L. Gole, *Nano Lett.*, 2003, **3**, 1049.
8 J. L. Gole, J. D. Stout, C. Burda, Y. Lou and X. Chen, *J. Phys. Chem. B*, 2004, **108**, 1230.
9 X. Chen, Y. Lou, A. C. S. Samia, C. Burda and J. L. Gole, *Adv. Funct. Mater.*, 2005, **15**, 41.
10 S. M. Prokes, J. L. Gole, X. Chen, C. Burda and W. E. Carlos, *Adv. Funct. Mater.*, 2005, **15**, 161.
11 A. Ghicov, J. M. Macak, H. Tsuchiya, J. Kunze, V. Haeablein, L. Frey and P. Schumaki, *Nano Lett.*, 2006, **6**, 1080.
12 G. Ghicov, J. M. Macak, H. Tsuchiya, J. Kunze, V. Haeablein, S. Kleber and P. Schumuki, *Chem. Phys. Lett.*, 2006, **419**, 426.
13 P. R. Vitiello, J. M. Macak, A. Ghicov, J. Tsuchiya, L. F. P. Dick and P. Schmuki, *Electrochem. Commun.*, 2006, **8**, 544.

14 R. Nakamura, T. Tanaka and Y. Nakato, *J. Phys. Chem. B*, 2004, **108**, 10617.
15 T. Lindgren, J. M. Mwabora, E. Avendano, J. Jonsson, C. G. Granqvist and S. E. Lindquist, *J. Phys. Chem. A*, 2003, **107**, 5709.
16 S. Livraghi, M. C. Paganini, E. Giamello, A. Selloni, C. D. Valentin and G. Pacchioni, *J. Am. Chem. Soc.*, 2006, **128**, 15666.
17 N. Serpone, *J. Phys. Chem. B*, 2006, **110**, 24287.
18 V. N. Kuznetsov and N. Serpone, *J. Phys. Chem. B*, 2006, **110**, 25203.
19 A. V. Emeline, N. V. Sheremetyeva, N. V. Khomchenko, V. K. Ryabchuk and N. Serpone, *J. Phys. Chem. C*, 2007, **111**, 11456.
20 T. Kasuga, M. Hiramatsu, A. Hoson, T. Sekino and K. Niihara, *Langmuir*, 1998, **14**, 3160.
21 J. J. Yang, Z. S. Jin, X. D. Wang, W. Li, J. W. Zhang, S. L. Zhang, X. Y. Guo and Z. J. Zhang, *Dalton Trans.*, 2003, **20**, 3898.
22 C. C. Tsai and H. Teng, *Chem. Mater.*, 2006, **18**, 367.
23 S. L. Zhang, J. F. Zhou, Z. J. Zhang, A. V. Vorontsov and Z. S. Jin, *Chin. Sci. Bull.*, 2000, **45**, 1533.
24 Y. Wang, C. X. Feng, Z. S. Jin, J. W. Zhang, J. J. Yang and S. L. Zhang, *J. Mol. Catal. A: Chem.*, 2006, **260**, 1.
25 M. Zhang, Z. S. Jin, J. W. Zhang, X. Y. Guo, J. J. Yang, W. Li, X. D. Wang and Z. J. Zhang, *J. Mol. Catal. A: Chem.*, 2004, **217**, 203.
26 S. Kumar, A. G. Fedorov and J. L. Gole, *Appl. Catal., B*, 2005, **57**, 93.
27 C. D. Valentin, G. Pacchioni, A. Selloni, S. Livraghi and E. Giamello, *J. Phys. Chem. B*, 2005, **109**, 11414.
28 W. W. Wendlandt and H. G. Hecht, *Reflectance Spectroscopy*, Wiley Interscience, New York, 1966.
29 J. R. Anderson and K. C. Pratt, *Introduction to Characterization and Testing of Catalysts*, Academic Press, Australia, 1985.
30 S. L. Zhang, W. Li, Z. S. Jin, J. J. Yang, J. W. Zhang, Z. L. Du and Z. J. Zhang, *J. Solid State Chem.*, 2004, **177**, 1365.
31 S. Sato, R. Nakamura and S. Abe, *Appl. Catal., A*, 2005, **284**, 131.
32 J. A. Rodriguez, T. Jirsak, J. Dvorak, S. Sambasivan and D. Fischer, *J. Phys. Chem. B*, 2000, **104**, 319.
33 Y. Suda, H. Kawasaki, T. Ueda and T. Ohshima, *Thin Solid Films*, 2004, **453**, 162.
34 N. C. Saha and H. G. Tompkins, *J. Appl. Phys.*, 1992, **72**, 3072.
35 Y. Nosaka, M. Matsushita, J. Nishino and A. Y. Nosaka, *Sci. Technol. Adv. Mater.*, 2005, **6**, 143.
36 S. W. Yang and L. Gao, *J. Am. Ceram. Soc.*, 2004, **87**, 1803.
37 O. Diwald, T. L. Thompson, T. Zubkov, E. G. Goralski, S. D. Walck and J. T. Yates Jr, *J. Phys. Chem. B*, 2004, **108**, 6004.
38 T. Tachikawa, M. Fujitsuka and T. Majima, *J. Phys. Chem. C*, 2007, **111**, 5259.
39 *Handbook of X-Ray Photoelectron Spectroscopy*, ed. C. D. Wagner, W. M. Riggs, I. E. Davis, J. F. Moulder and G. E. Muilenberg, Perkin-Elmer Corporation, Physical Electronics Division, Eden Prairie, MN, 1979.
40 J. M. Hermann, J. Disdier and P. Pichat, *Chem. Phys. Lett.*, 1984, **108**, 618.
41 W. Choi, A. Termin and M. R. Hoffmann, *J. Phys. Chem.*, 1994, **98**, 13669.
42 M. R. Hoffmann, S. T. Martin, W. Choi and D. W. Bahnemann, *Chem. Rev.*, 1995, **95**, 69.
43 D. Dvoranova, V. Brezova, M. Mazur and M. A. Malati, *Appl. Catal., B*, 2002, **37**, 91.
44 M. Anpo and M. Takeuchi, *J. Catal.*, 2003, **216**, 505.
45 T. Ihara, Y. Ikeuchi, M. Miyoshi, M. Ando, S. Sugihara and Y. Iriyama, *J. Mater. Sci.*, 2001, **36**, 4201.
46 K. Takeuchi, I. Nakamura, O. Matsumoto, S. Sugihara, M. Ando and T. Ihara, *Chem. Lett.*, 2000, 1354.
47 D. C. Cronemeyer, *Phys. Rev.*, 1959, **113**, 1222.
48 M. Z. Su, *Solid State Chemistry, An Introduction*, Peking University Press, Beijing, 1987 (Chinese).
49 Q. Y. Li, J. W. Zhang, Z. S. Jin, D. G. Yang, X. D. Wang, J. J. Yang and Z. J. Zhang, *Electrochem. Commun.*, 2006, **8**, 741.
50 E. Serwicka, M. W. Schlierkamp and R. N. Schindler, *Z. Naturforsch., A: Phys., Phys. Chem., Kosmophys.*, 1981, **36**, 226.
51 E. Serwicka, *Colloids Surf.*, 1985, **13**, 287.
52 I. Nakamura, N. Negishi, S. Kutsuna, T. Ihara, S. Sugihara and K. Takeuchi, *J. Mol. Catal. A: Chem.*, 2000, **161**, 205.
53 L. Qian, Z. S. Jin, J. W. Zhang, Y. B. Huang, Z. J. Zhang and Z. L. Du, *Appl. Phys. A: Mater. Sci. Process.*, 2005, **80**, 1801.
54 Q. Y. Li, X. D. Wang, Z. S. Jin, D. G. Yang, S. L. Zhang, X. Y. Guo, J. J. Yang and Z. J. Zhang, *J. Nanopart. Res.*, 2007, **5** 951.
55 X. D. Wang, J. J. Yang, H. Y. Yin, Z. J. Zhang and Z. S. Jin, *Photogr. Sci. Photochem.*, 2002, **20**, 424 (Chinese).
56 R. D. Iyengar, M. Codell, J. S. Karra and J. Turkevich, *J. Am. Chem. Soc.*, 1966, **88**, 5055.
57 S. Fukuzawa, K. M. Sancier and T. Kwan, *J. Catal.*, 1968, **11**, 364.
58 R. D. Iyengar and R. J. Kellerman, *J. Colloid Interface Sci.*, 1971, **35**, 424.
59 S. Livraghi, A. Votta, M. C. Paganini and E. Giamello, *Chem. Commun.*, 2005, **4**, 498.